

# Determination of Tyrosine in Artificial Urine Using a Screen-Printed Electrode Modified with tetrathiafulvalene–tetracyanoquinodimethane/ionic Liquid Conductive Gel

Xiaoping Zhang<sup>2</sup>, Xiatong Li<sup>1</sup>, Xinyue Pei<sup>1</sup>, Ting Shu<sup>1</sup>, Qing Min<sup>1</sup>, Shi Wang<sup>1,\*</sup>

<sup>1</sup> School of Pharmacy, Hubei University of Science and Technology, Xianning 437100, China

<sup>2</sup> Hepatobiliary pancreas surgery, Xianning Central Hospital, The First Affiliated Hospital Of Hubei University of Science and Technology, Xianning 437100, China.

\*E-mail: [wangshi413@gmail.com](mailto:wangshi413@gmail.com)

Received: 9 April 2020 / Accepted: 16 June 2020 / Published: 10 August 2020

In this study, the screen-printed electrode (SPE) was developed for detection of tyrosine based on tetrathiafulvalene-tetracyanoquinodimethane/ionic liquid conductive gel. The electrocatalytic behavior of TTF–TCNQ/ionic liquid gels was investigated by cyclic voltammetry analyses. [BMIM][PF<sub>6</sub>] gel based SPE (TTF-TCNQ/[BMIM][PF<sub>6</sub>]-SPE) allowed square wave voltammetry detection of tyrosine (Tyr). The optimum experimental conditions for the detection were explored, and the currents of Tyr presented a good linear property with the increasing of the concentrations. The linear ranges of Try were determined to be  $1 \times 10^{-7}$ – $2.0 \times 10^{-5}$  M and the minimum detection limit was  $4 \times 10^{-8}$  M. Furthermore, the TTF-TCNQ/[BMIM][PF<sub>6</sub>]/SPE was successfully used for the detection of Try in the artificial urine samples.

**Keywords:** tyrosine; screen-printed electrode; tetrathiafulvalene–tetracyanoquinodimethane; ionic liquid

## 1. INTRODUCTION

Tyrosine (Tyr) is a conditionally essential amino acid, which is involved in the construction of almost all proteins in the human body [1]. It is also a significant precursor of several neurotransmitters, such as dopamine, norepinephrine, epinephrine and other catecholamines [2]. Tyr is essential for humans to establish and maintain nutritional balance, due to its important role in biological systems [3]. Increased Tyr levels may induce Parkinson's disease, depression, and mood disorders, while Tyr deficiency can cause albinism and alkaptonuria [4, 5]. Tyr and its metabolites are associated with inborn error diseases[6], and changes in Tyr concentration are related to atherosclerosis [7] and lung diseases [8].

Because alteration of Tyr concentration is closely related to certain human diseases, it is important to determine Tyr in human fluids (such as plasma and urine). Therefore, simple and fast methods are needed to satisfy the demand for Tyr determination in clinical analysis.

Numerous techniques like liquid chromatographic-tandem mass spectrometry (LC-MS) [9], high performance liquid chromatography (HPLC) [10, 11], chemiluminescence [12], spectrophotometry [13, 14], fluorimetry [15] and capillary electrophoresis [16] have been used to determine Tyr. However, these methods have some disadvantages, such as time-consuming and complicated sample preparation procedures, which makes them unsuitable for routine analysis. The screen printing technology has overtaken the traditional techniques in analyzing biological samples due to its low cost, large scale capacity and facile operation [17]. The screen-printed electrodes (SPEs) are versatile, easy to use analytical tools, and also suitable for miniaturization [18]. The electrochemical behavior of Tyr shows a completely irreversible process with an oxidation potential of 728 mV at the glassy carbon electrode [19]. Various electrocatalysts have been modified on the electrode surface for improving their electrochemical performance, such as graphene nanowalls [20], Graphene oxide/ZnO nano composite [21], conducting polymer/Au nanocomposite [22], etc.

Tetrathiafulvalene-tetracyanoquinodimethane (TTF-TCNQ) is a conductive organic complex salt characterized by the partial transfer of electrons from the donor to the acceptor molecule. TTF-TCNQ offers many advantages, such as high electronic conductivity and easy tailoring of its crystal shape and size [23]. The unique electrical properties of TTF-TCNQ have prompted researches on its utilization as electrode material for direct electron transfer with many electroactive compounds or as mediators in various electrode construction [24, 25]. On the other hand, ionic conductivity, hydrophobicity, high viscosity, and biocompatibility are characteristics of ionic liquids, which make them attractive for electrode modification [26]. Novel electronically and ionically conductive gels are fabricated by mixing ionic liquids (IL) with TTF-TCNQ complex [27]. Similar to the carbon nanotube-ionic liquid gel, the formation of the gel is related to the  $\pi$ - $\pi$  and Coulombic interaction between TTF-TCNQ and ILs [28]. TTF-TCNQ/ionic liquid gels exhibit high electrical conductivity and are very promising electrode materials [29].

With this background, a novel, sensitive and convenient electrochemical method was developed in this work, which could find its successful application in the determination of Tyr in artificial urine samples. The screen-printed electrode was comprised of carbon counter electrode, Ag/AgCl reference electrode and TTF-TCNQ/[BMIM][PF<sub>6</sub>] gel modified carbon working electrode. The prepared TTF-TCNQ/[BMIM][PF<sub>6</sub>] gel could be used as an electron conductor and catalytic mediator for Try oxidation, leading to a sensitive Try detection. To the best of our knowledge, no study has been reported on the determination of Tyr in artificial urine samples using TTF-TCNQ/ionic liquid gels modified screen printed electrode.

## 2. EXPERIMENTAL

### 2.1 Reagents and instruments

The tetrathiafulvalene (TTF), tetracyanoquinodimethane (TCNQ), tetrathiafulvalene-

tetracyanoquinodimethane (TTF-TCNQ) were of analytical reagent grade and purchased from Sigma-Aldrich. 1-Butyl-3-methylimidazolium tetrafluoroborate ([BMIM][BF<sub>4</sub>]), 1-butyl-3-methylimidazolium hexafluorophosphate ([BMIM][PF<sub>6</sub>]), 1-Ethyl-3-methylimidazolium thiocyanate ([EMIM][SCN]) and 1-ethyl-3-methylimidazolium dicyanamide ([EMIM][DCA]) were all supplied by Shanghai Chengjie Chemical Co., Ltd. Artificial urine was purchased from Chang Feng technology. 0.1 M Phosphate buffer (PBS) was used as supporting electrolyte. The pH of PBS was adjusted by using 1.0 M hydrochloric acid (HCl) or 1.0 M sodium hydroxide (NaOH). All chemicals and solvents used were of analytical grade. Ultrapure water from Millipore was used in all experiments.

All electrochemical measurements were performed using a CHI660E electrochemical workstation (CH Instrument, China). Scanning electron microscope (Zeiss SIGMA, British) was obtained for the morphological analysis of the bare and modified SPEs. SEM images were recorded by Signal A= InLens mode, WD= 4.8 mm, EHT= 5.00 kV, Mag= 100X. (Scale bar: 100  $\mu$ m) and Mag= 1.00 KX (Scale bar: 10  $\mu$ m).

## 2.2. Preparation of modified screen-printed electrode

According to the previous research [30], the SPE were produced as the three electrode system with carbon working electrode (WE), carbon counter electrode (CE) and Ag/AgCl reference electrode (RE) (Figure 1). The WE of the screen-printed substrate was gently rinsed with ultrapure water to ensure the removal of any extraneous material.

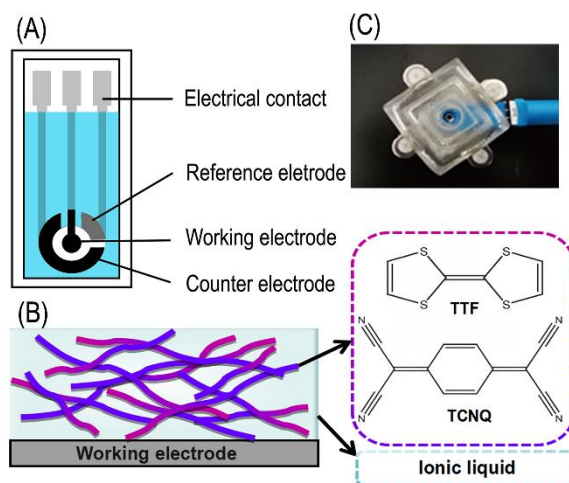


**Figure 1.** (A) The structure of screen printed electrode(SPE), (B) Schematic illustration of TTF–TCNQ/IL gels modified WE, (C) Image of the SPE and laboratory-made cell.

After drying, TTF–TCNQ/IL gels modified SPE was developed as following. First, the TTF–TCNQ/IL gels were prepared by grinding TTF–TCNQ in different ionic liquids. In a typical experiment, 1 mL IL was added to 20 mg TTF–TCNQ into a mortar and the mixture was ground for 5 min. Because TTF and TCNQ have almost the same molecular weight, the ratio of TTF:TCNQ remains approximately

1:1.

Next, the TTF–TCNQ/IL/SPE was prepared by casting of 2  $\mu$ l TTF–TCNQ/IL gels on the surface of WE. Then, it was set into a dry oven at 37 °C for 20 h. The TCNQ/IL and TTF/IL gels were prepared by grinding 10 mg of TCNQ and TTF in IL, respectively. Preparation of the TCNQ/IL/SPE and TTF/IL/SPE were performed by casting of 2  $\mu$ l solutions TCNQ/IL and TTF/IL respectively, on the surface of WE and left to dry at 37 °C for 20 h in dry oven. Other kinds of modified SPE including TTF–TCNQ/acetonitrile solution modified SPE (TTF–TCNQ/ACN/SPE) etc. were prepared by the similar procedure and used for comparison.

### 2.3. Electrochemical Measurements

The appropriate amounts of Tyr were added to 0.1M PBS (pH 1.0) buffer solution in laboratory-made cell. Cyclic voltammetry and square wave voltammetry experiments were recorded over the potential range from -0.8 to +1.2 V. All experiments were carried out at room temperature.

### 2.4. Analysis of artificial urine sample

The artificial urine was detected for analysis without any pretreatment. 1 mL artificial urine was diluted to 1 mL in electrolytic cell by 0.1 M PBS (pH 1.0). Then, the diluted artificial urine was directly added on the SPE surface as a droplet (200  $\mu$ L) and electrochemical scan was performed immediately.

## 3. RESULTS AND DISCUSSION

### 3.1. Cyclic voltammetry studies on TTF–TCNQ/IL/SPE

[EMIM][SCN], [EMIM][DCA], [BMIM][BF<sub>4</sub>] and [BMIM][PF<sub>6</sub>] salts were chosen to study the effect of the anion and side chains on the TTF-TCNQ/IL gels. Because the anion and the side chain of imidazole can significantly affect the properties of ILs [27]. Cyclic voltammetry was used to compare the electrochemical behavior of TTF-TCNQ/[BMIM][PF<sub>6</sub>]/SPE, TTF-TCNQ/[EMIM][SCN]/SPE, TTF-TCNQ/[EMIM][DCA]/SPE and TTF-TCNQ/[BMIM][BF<sub>4</sub>]/SPE. The CV studies exhibited clearly distinguished oxidation and reduction peaks for the TTF-TCNQ/[BMIM][PF<sub>6</sub>]/SPE comparing with other three types of TTF–TCNQ/IL/SPEs (Figure 2).

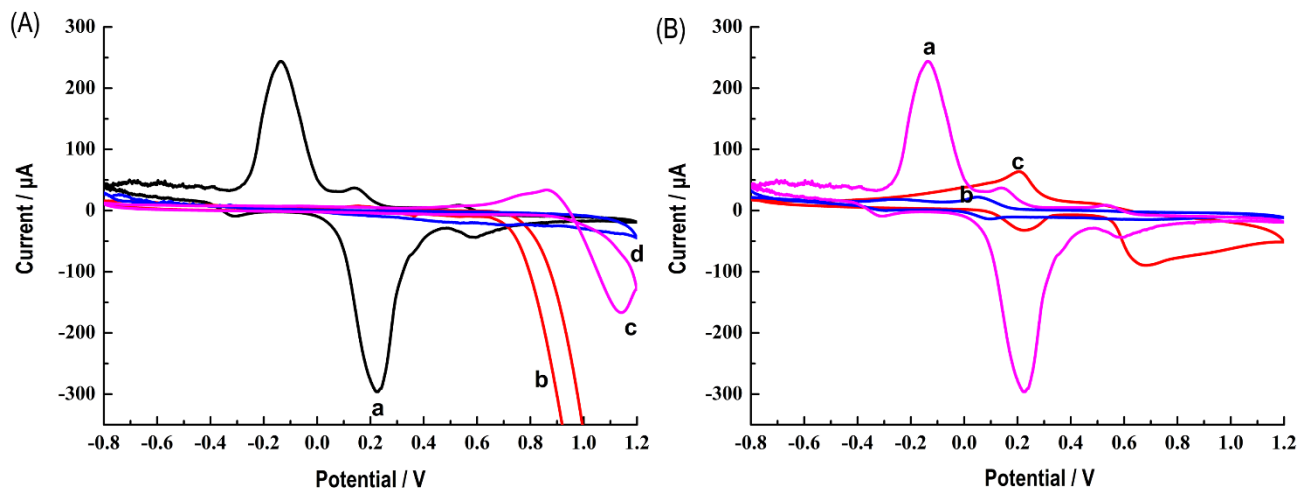


**Figure 2.** Cyclic voltammograms for (A). TTF-TCNQ/[BMIM][PF<sub>6</sub>]/SPE (a), TTF-TCNQ/[EMIM][SCN]/SPE(b), TTF-TCNQ/[EMIM][DCA]/SPE(c), TTF-TCNQ/[BMIM][BF<sub>4</sub>]/SPE (d). B. TTF-TCNQ/[BMIM][PF<sub>6</sub>]/SPE (a), TCNQ/[BMIM][PF<sub>6</sub>]/SPE (b) and TTF/[BMIM][PF<sub>6</sub>]/SPE (c). Scan rate = 20 mV/s, pH = 1.

In TTF-TCNQ, TTF is an electron donor and TCNQ is an acceptor. TCNQ can undergo two redox transformations, which are converted to the monovalent (TCNQ<sup>-</sup>) and subsequently to the divalent (TCNQ<sup>2-</sup>) radical anions. TTF can undergo two redox transformations, which are converted to the TTF<sup>+</sup> and the TTF<sup>2+</sup> radical cations, respectively. According to the literature [31], the TTF and TCNQ species can be generated from the surface of TTF-TCNQ by potential induced salt decomposition during the electrochemical tests and can also react to reform. So the oxidation process of TTF-TCNQ/[BMIM][PF<sub>6</sub>]/SPE could be associated with the production of TTF<sup>2+</sup>, TTF<sup>+</sup> cation and TCNQ<sup>0</sup>, while the reduction process could be based on the anion TCNQ<sup>2-</sup>, TCNQ<sup>-</sup> and TTF<sup>0</sup> [29]. The CVs for TTF-TCNQ/[BMIM][PF<sub>6</sub>]/SPE, TCNQ/[BMIM][PF<sub>6</sub>]/SPE and TTF/[BMIM][PF<sub>6</sub>]/SPE were tested for more information. As can be seen in Figure 2B, a redox process at 0.2 V, assigned to the TTF<sup>0</sup>/TTF<sup>+</sup> couple, occurs at TTF/[BMIM][PF<sub>6</sub>]/SPE. The TTF<sup>+</sup>/TTF<sup>2+</sup> exhibits an oxidation peak at 0.68V and a reduction peak at around 0.49V. The TTF<sup>2+</sup> species acts at more positive potentials but they are less stable and easily decomposed [31]. It can be seen that CV of TCNQ/[BMIM][PF<sub>6</sub>]/SPE exhibits a pair of redox peaks at -0.30V and -0.26V, respectively. These peaks can be assigned to the redox couple TCNQ<sup>2-</sup>/TCNQ<sup>-</sup>. Another well-defined pair of redox peaks can be observed at 0.095V and 0.05V, respectively. This process is assigned to the TCNQ<sup>-</sup>/TCNQ<sup>0</sup> redox couple. The CV of TTF-TCNQ/[BMIM][PF<sub>6</sub>]/SPE is characterized by clearly developed three pairs of redox peaks. The reduction and oxidation of TTF or TCNQ occur at different potentials as compared with that of the TTF-TCNQ [25]. Based on its position and shape, the pair of redox peaks at 0.58V and 0.53V, respectively, can be assigned to the TTF<sup>+</sup>/TTF<sup>2+</sup> couple. Based on this observation, it is assumed that the reduction peak at 0.13V is due to the TTF<sup>0</sup>/TTF<sup>+</sup> couples. However, the anodic peak at 0.22V is attributed both to the TTF<sup>0</sup>/TTF<sup>+</sup> and TCNQ<sup>-</sup>/TCNQ<sup>0</sup> couples. It is difficult to distinguish between these processes since they are superimposed in the potential range. This also implies that the the small anodic peak at -0.33V

is due to  $\text{TCNQ}^{2-}$  oxidation to  $\text{TCNQ}^-$ , and the corresponding reduction peak appeared at  $-0.14\text{V}$  can be attributed both to the  $\text{TCNQ}^{2-}/\text{TCNQ}^-$  and the  $\text{TCNQ}^-/\text{TCNQ}^0$  couples.

The CV studies exhibited well-defined electrochemical behavior for the TTF-TCNQ/[BMIM][PF<sub>6</sub>]/SPE comparing with TTF-TCNQ/[EMIM][SCN]/SPE, TTF-TCNQ/[EMIM][DCA]/SPE and TTF-TCNQ/[BMIM][BF<sub>4</sub>]/SPE. Therefore, [BMIM][PF<sub>6</sub>] was selected for the fabrication of the TTF-TCNQ/[BMIM][PF<sub>6</sub>]/SPE.

### 3.2. Characterization of modified SPEs

The SEM images of working electrodes from bare and modified SPEs are shown in Figure 3 A-H. The morphology of TTF/ACN/SPE and TTF-TCNQ/ACN/SPE was investigated. In both cases rectangle-like and plate-like shaped crystals of TTF and TCNQ are clearly visible (Figure 3 A-B), similar to those reported in the literature [32].

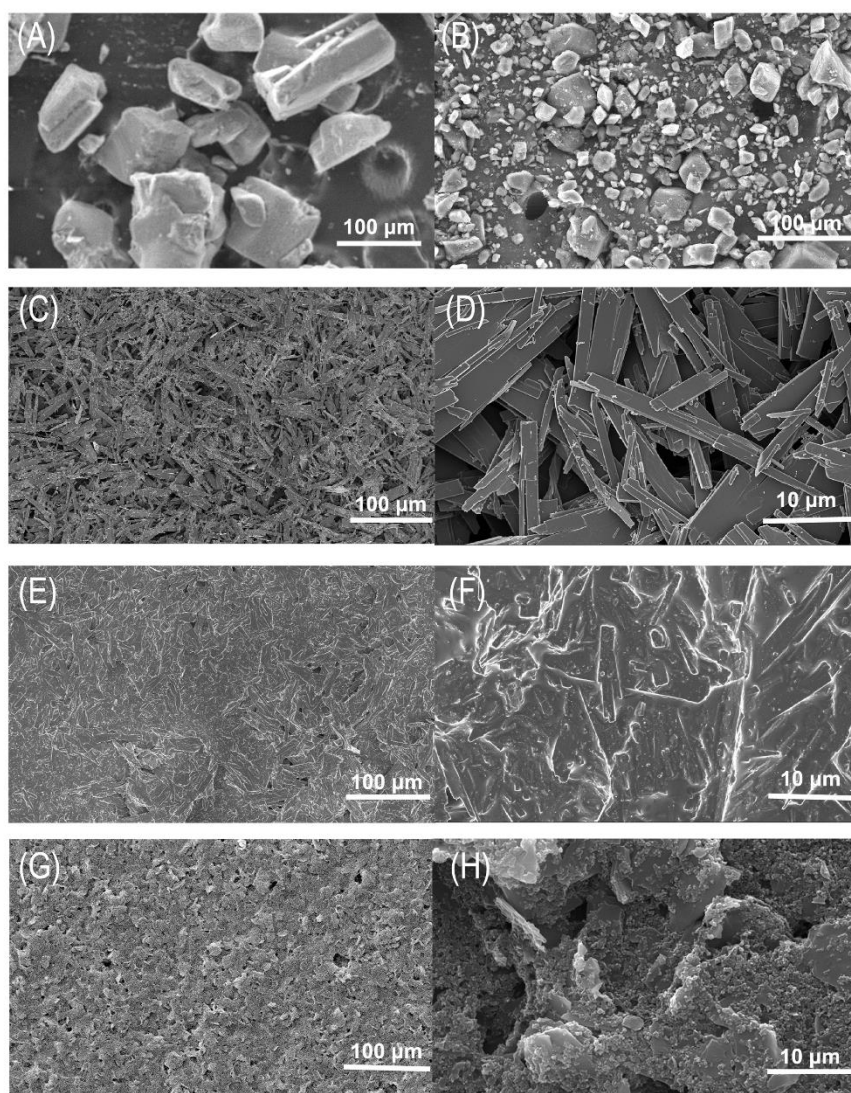


**Figure 3.** SEM images of TTF/ACN/SPE (A), TCNQ/ACN/SPE (B), TTF-TCNQ/ACN/SPE (C-D), TTF-TCNQ/[BMIM][PF<sub>6</sub>]/SPE (E-F) and bare SPE (G-H).

It can be seen from Figure 3 C-D that the microstructure of the crystals of the TTF-TCNQ composite is shown in the TTF-TCNQ/ACN, while the Figure 3 E-F show that the TTF-TCNQ/[BMIM][PF<sub>6</sub>] gel has a good dispersion structure in the crystal. The TTF-TCNQ/[BMIM][PF<sub>6</sub>] gel is well distributed on the surface, which can provide a relatively smooth and stable electrode surface, rather than microcrystalline deposits of TTF-TCNQ salts observed in the TTF-TCNQ/ACN [33]. The surfaces of bare SPE, as shown in Figure 3 G-H, show that the carbon surface is covered with a great content of graphite particles. The final structure of TTF-TCNQ/[BMIM][PF<sub>6</sub>]/SPE is significantly larger than the geometric area of bare SPE. The immobilization of the Tyr over such a surface results in its uniform distribution.

### 3.3. Electrochemical activity of Tyr at the TTF-TCNQ/[BMIM][PF<sub>6</sub>]/SPE

Figure 4A shows the results obtained by investigation of the CVs of TTF-TCNQ/[BMIM][PF<sub>6</sub>]/SPE in 0.1 M pH 1.0 PBS containing 1mM Try. In the PBS, three pairs of redox peaks corresponding to the reaction of TTF and TCNQ species are observed in Fig. 4A(b). When 1mM Try was added into the PBS (curve c, Figure 4A), the anodic and cathodic peaks enhanced obviously, especially the anodic peak at 0.22V and cathodic peak appeared at -0.14V. And the peak potentials both shifted slightly. One explanation for the increase in peak current is that Tyr might chemically reduce TCNQ to TCNQ<sup>-</sup>, and TCNQ<sup>-</sup> is electrochemically oxidized to TCNQ. As a result, an increase in the anodic peak current is observed [34]. At last, anodic and cathodic peaks all are enhanced. When the same experiments were performed using bare SPE, as shown in Figure 4A(a), no response for Tyr was observed within the studied potential range. The comparison results showed that TTF-TCNQ/[BMIM][PF<sub>6</sub>] exhibited an unexpected electrocatalytic activity for Tyr oxidation.

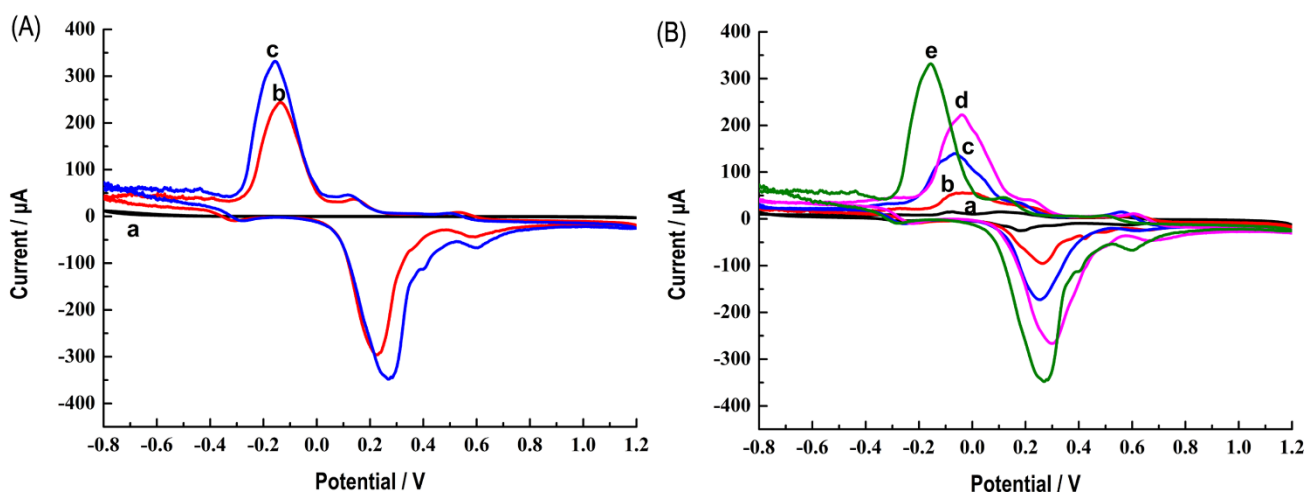


**Figure 4.** (A) Cyclic voltammograms obtained for bare SPE in 0.1 M PBS (pH 1) containing 1mM Tyr (a), and TTF-TCNQ/[BMIM][PF<sub>6</sub>]/SPE in absence (b) and presence (c) of 1 mM Tyr in 0.1 M PBS (pH 1). Scan rate: 20 mV/s. (B) Cyclic voltammograms of 1 mM Tyr in 0.1 M PBS (pH 1) at different concentration of TTF-TCNQ/[BMIM][PF<sub>6</sub>] gel modified SPEs: 1, 5, 10, 20 mg/mL (a to d). Scan rate: 20 mV/s.

In order to optimize the TTF-TCNQ/[BMIM][PF<sub>6</sub>]/SPE preparation, the appropriate amount of the TTF-TCNQ in TTF-TCNQ/[BMIM][PF<sub>6</sub>] gel was optimized, and the obtained results are shown in Figure 4B. 1-5 mg/mL concentration of TTF-TCNQ/[BMIM][PF<sub>6</sub>] gel were found to have low stability during electrochemical assays. Increasing the amount of TTF-TCNQ in TTF-TCNQ/[BMIM][PF<sub>6</sub>] gel could lead to an enhancement of the electrocatalytic properties and consequently to an improvement of the current. As the TTF-TCNQ amount was increased beyond 20 mg/mL, the current was decreased. Therefore, the highest peak current was achieved with the composition of 20 mg/mL TTF-TCNQ/[BMIM][PF<sub>6</sub>] gel.

### 3.4. Influences of pH

The influence of the pH values of the supporting electrolyte on the behavior of Tyr at the TTF-TCNQ/[BMIM][PF<sub>6</sub>]/SPE was investigated by CV. The effect of pH on electrode response was investigated in the range pH 1-10. The results indicated that acidic solutions respond better to Tyr than alkaline solutions. And the peak currents increased with pH in the range from pH 5 down to pH 1. Various supporting electrolytes were tested, and phosphate buffer was found to have the best response. According to the literature [35], a reasonable explanation for this behavior is the interaction between the cations in the buffer and TTF-TCNQ complex. Therefore, pH 1 PBS was chosen for the following experiments.

### 3.5 Influence of the scan frequency and potential increment

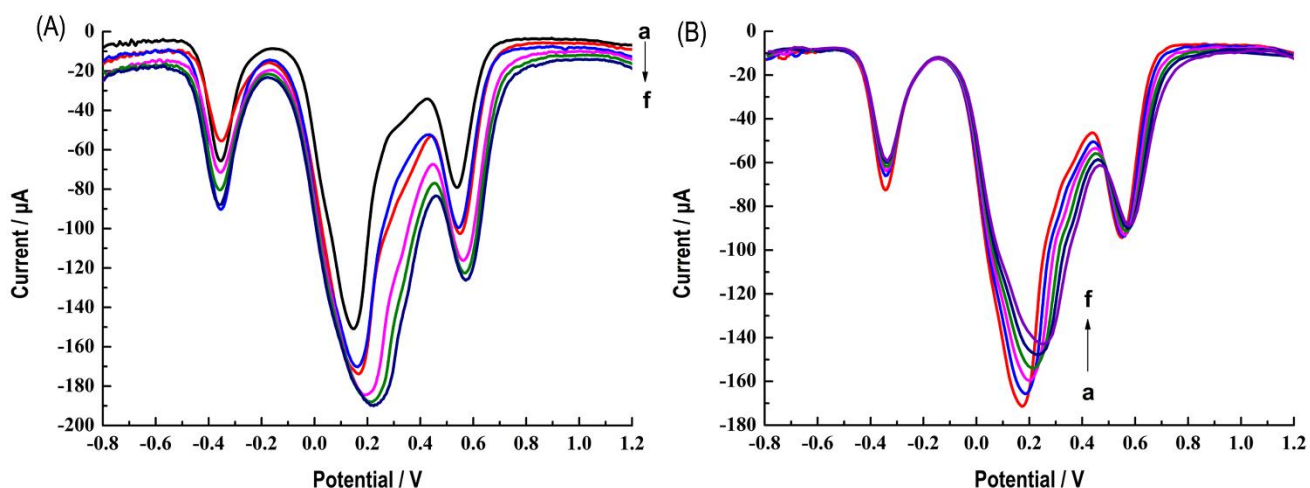


**Figure 5.** Square wave voltammograms of 0.1 mM Tyr at TTF-TCNQ/[BMIM][PF<sub>6</sub>]/SPE in different frequency (a→f: 5, 10, 15, 20, 25 and 30 Hz) (A) and in different potential increment (a→f: 6, 8, 10, 12, 14 and 16 mV) (B).

SWV was further employed to increase the sensitivity of the measured signal. The properties of SWV were compared in order to find a more sensitive method for Tyr determination. The effect of different scan frequencies and potential increments were studied for the determination of 0.1 mM Tyr.

As can be seen from Figure 5A, in the range of 5-10 Hz, the anodic peak currents around 0.2 V were significantly enhanced in the range of 5–10 Hz and gradually decreased in the range of 15–30 Hz. From Figure 5B, it can be seen that the peak currents increased first and then decreased with increasing frequency in the range of 6–16 mV. The anodic peak current around 0.2 V reached the maximum at 6 mV. Therefore, 10 Hz and 6 mV were selected for further SWV determination.

### 3.6 Calibration curve and limit detection

Various concentrations of Tyr were examined under optimal condition by SWV. As shown in Figure 6, the calibration equation was obtained in the range of  $1.0 \times 10^{-7}$  to  $2.0 \times 10^{-5}$  M,  $I_p = 3.39C + 22.57$  ( $R = 0.995$ ). The detection limit was found to be  $0.4 \times 10^{-7}$  M ( $S/N = 3.0$ ).

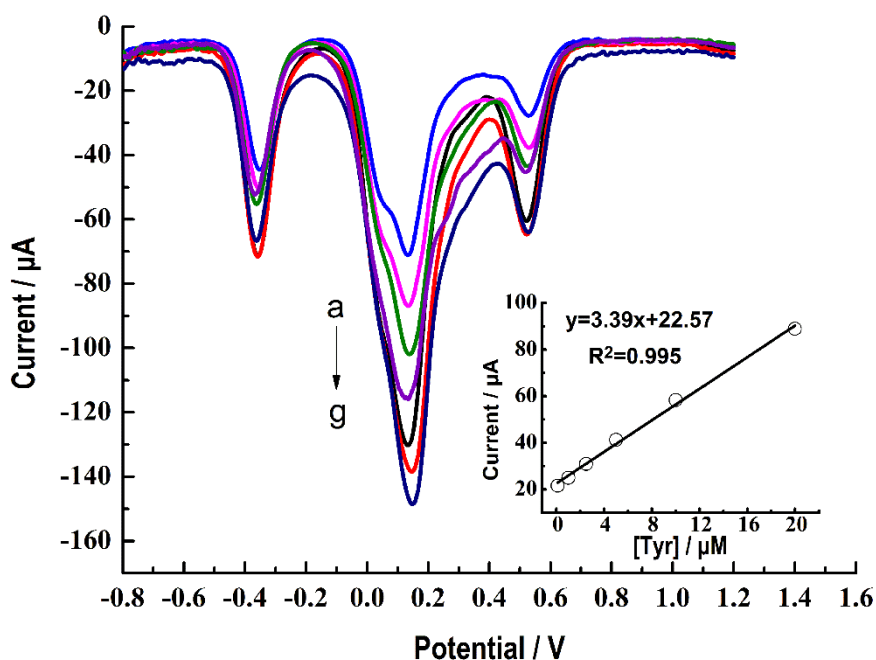


**Figure 6.** Square wave voltammograms of different concentrations of Tyr in 0.1 M PBS (pH 1.0). a→g: 0, 0.1, 1, 2.5, 5, 10 and 20 µM, respectively. The inner picture shows the calibration curve between the relative SWV peak current changes and the concentrations of Tyr.

The developed TTF-TCNQ/[BMIM][PF<sub>6</sub>]/SPE was compared with other modified electrodes reported in the literature, and the corresponding values of the evaluation parameters were presented. As can be seen in the table 1, GCE is the most common type of electrode for voltammetric determination of Tyr. Au nanoparticles@metal organic framework/polythionine/molecularly imprinted polymer [36], poly (amidoamine)/multi-walled carbon nanotube nanocomposite [37], conducting polymer/Au nanocomposite [22], nano-structured ultrathin g-C<sub>3</sub>N<sub>4</sub>/Ag nanoparticle hybrids [38], gold matrices [39], 3-amino-5-mercapto-1,2,4-triazole [40], graphene ganosheets gomposite [41], reduced graphene oxide

[42] and other materials were used to modify GCE to increase the selectivity and sensitivity of Tyr. And other electrodes included graphene nanowalls coated tantalum electrode [20], grapheme oxide/ZnO nanorods nano composite modified graphite screen-printed electrode [21], etc. It can be seen that compared with other electrodes, the proposed TTF-TCNQ/[BMIM][PF<sub>6</sub>]/SPE presented a similar linear response range and detection limit. Although some modified electrodes showed better sensitivity than TTF-TCNQ/[BMIM][PF<sub>6</sub>]/SPE, these methods suffered from extensive and complex pre-treatment steps of analysis.

**Table 1.** Comparison of different modified electrodes for Tyr determination

Modified electrode	The linear range (M)	Detection limits (M)	Reference
MIP/pTH/Au@ZIF-67/GCE	$1 \times 10^{-8} - 4 \times 10^{-6}$	$7.9 \times 10^{-10}$	[36]
Hemin/PAMAM/MCNT/GCE	$1 \times 10^{-7} - 2.88 \times 10^{-5}$	$1.0 \times 10^{-8}$	[37]
GR/ZnO/GSPE	$1 \times 10^{-6} - 8 \times 10^{-4}$	$3.4 \times 10^{-7}$	[21]
Graphene/Ta	$8 \times 10^{-6} - 1 \times 10^{-4}$	$8.0 \times 10^{-7}$	[20]
NiO/CNTs/DPID/CPEs	$5 \times 10^{-6} - 7.5 \times 10^{-4}$	$1.0 \times 10^{-6}$	[40]
PABSA/Au/GCE	$1 \times 10^{-6} - 1 \times 10^{-4}$	$4.0 \times 10^{-7}$	[22]
UT-g-C <sub>3</sub> N <sub>4</sub> /Ag/GCE	$1 \times 10^{-6} - 1.5 \times 10^{-4}$	$1.4 \times 10^{-7}$	[38]
AuNPs/GCE	$4 \times 10^{-6} - 1 \times 10^{-3}$	$1.3 \times 10^{-6}$	[39]
p-AMTa/GCE	$5.0 \times 10^{-8} - 1.0 \times 10^{-4}$	$1.9 \times 10^{-10}$	[40]
GNS/GCE	$5 \times 10^{-6} - 1.2 \times 10^{-4}$	$2.0 \times 10^{-8}$	[41]
hemin-rGO/GCE	$5 \times 10^{-7} - 2 \times 10^{-5}$	$7.5 \times 10^{-8}$	[42]
TTF-TCNQ/IL/SPE	$1 \times 10^{-7} - 2.0 \times 10^{-5}$	$4.0 \times 10^{-8}$	This work

### 3.7. Interference, reproducibility and stability

In order to evaluate the selectivity of TTF-TCNQ/[BMIM][PF<sub>6</sub>]/SPE, in the presence of 10 μM Tyr, a variety of interfering substances were studied in biological samples, such as vitamin C, glucose, urea, uric acid, alanine, glycine, Histidine, lysine, serine, etc. The results showed that 100 times of glucose, ascorbic acid, urea, uric acid, and 20 times of alanine, glycine, histidine, lysine, and serine did not interfere with Tyr. The results indicated that a relative error of largest amount was less than ±5%. These findings proved that the TF-TCNQ/[BMIM][PF<sub>6</sub>]/SPE had good selectivity for the determination of clinical samples.

The repeatability of the TTF-TCNQ/[BMIM][PF<sub>6</sub>]/SPE was investigated for responding to 1 μM Tyr. The relative standard deviation (RSD) of 6.8% (n = 5) was obtained. In addition, the stability of the TTF-TCNQ/[BMIM][PF<sub>6</sub>]/SPE was evaluated by recording its response to 1 μM Tyr. After being stored at room temperature and away from light for 2 weeks, the current response of the TTF-TCNQ/[BMIM][PF<sub>6</sub>]/SPE without significant change (error < 5%). The result demonstrated the reliability of the TTF-TCNQ/[BMIM][PF<sub>6</sub>]/SPE and its excellent reproducibility and high stability.

### 3.8. Determination of Tyr in artificial urine samples

The TTF-TCNQ/[BMIM][PF<sub>6</sub>]/SPE were used to the determination of Tyr in artificial urine samples by SWV. In order to evaluate the practical application of the fabricated TTF-TCNQ/[BMIM][PF<sub>6</sub>]/SPE, the standard addition method was employed to measure the concentration of Tyr in artificial urine samples. The TTF-TCNQ/[BMIM][PF<sub>6</sub>]/SPE showed good recoveries, which were 103–118% (Table 2). The good recoveries indicated that the TTF-TCNQ/[BMIM][PF<sub>6</sub>]/SPE can be well applied to the analysis of Tyr and without significant influence of the matrix.

**Table 2.** Determination of Tyr in artificial urine samples.

Sample	Added Tyr ( $\mu\text{mol/L}$ )	Founded Tyr ( $\mu\text{mol/L}$ )	Recovery (%)
1	0.10	0.10	103.00
2	5.00	5.49	109.80
3	10.00	11.80	118.00

## 4. CONCLUSIONS

In this work, the use of TTF-TCNQ/[BMIM][PF<sub>6</sub>] gel for development of Tyr sensors is presented. The electrochemical behavior of Tyr at TTF-TCNQ/[BMIM][PF<sub>6</sub>] gel modified SPE in PBS (pH 1) solution was investigated, and an analytical method for the determination of Tyr in artificial urine samples was successfully developed. Due to the unique structural and high electronic conductivity properties of TTF-TCNQ/[BMIM][PF<sub>6</sub>] gel, the TTF-TCNQ/[BMIM][PF<sub>6</sub>]/SPE could greatly improve the sensitivity of Tyr determination. The SWV peak currents were in a linear relationship with Tyr concentrations in the range of  $1.0 \times 10^{-7} - 2.0 \times 10^{-5}$  M, and the detection limit was  $4 \times 10^{-8}$  M. The TTF-TCNQ/[BMIM][PF<sub>6</sub>] modified SPE was very suitable and effective for determination of Tyr in artificial urine samples with good sensitivity, stability and selectivity. Further experiments are in progress to mix the TTF-TCNQ/[BMIM][PF<sub>6</sub>] gel into carbon ink for directly printing working electrode of SPE. By taking advantage of TTF-TCNQ/[BMIM][PF<sub>6</sub>] gel to change the electrochemical properties of the carbon ink, and to produce a new composite material that can improve the electrochemical performance of SPE.

## ACKNOWLEDGEMENTS

This work was supported by and the Educational Commission of Hubei Province of China (D20182802) and the National Natural Science Foundation of China (21804035).

## References

1. Z.-H. Yu and Z.-Y. Zhang, *Chem. Rev.*, 118 (2018) 1069.
2. M. S. Chow, B. E. Eser, S. A. Wilson, K. O. Hodgson, B. Hedman, P. F. Fitzpatrick and E. I. Solomon, *J. Am. Chem. Soc.*, 131 (2009) 7685.
3. E. Fernández-Espejo and C. Bis-Humbert, *Neurotoxicology*, 67 (2018) 178.

4. A. Gelenberg, C. Gibson and J. Wojcik, *Psychopharmacol. Bull.*, 18 (1982) 7.
5. J. S. Meyer, K. Welch, V. Deshmukh, F. Perez, R. Jacob, D. Haufrect, N. Mathew and R. Morrell, *J. Am. Geriatr. Soc.*, 25 (1977) 289.
6. E. Kvittingen, *J. Inherit. Metab. Dis.*, 14 (1991) 554.
7. T. Heitzer, T. Schlinzig, K. Krohn, T. Meinertz and T. Münzel, *Circulation*, 104 (2001) 2673.
8. H. Ischiropoulos, A. Al-Mehdi and A. B. Fisher, *Am J Physiol-lung C.*, 269 (1995) L158.
9. Y. Ishii, M. Iijima, T. Umemura, A. Nishikawa, Y. Iwasaki, R. Ito, K. Saito, M. Hirose and H. Nakazawa, *J. Pharm. Biomed. Anal.*, 41 (2006) 1325.
10. R. Kand'ár and P. Žáková, *J. Chromatogr. B*, 877 (2009) 3926.
11. X.-m. Mo, Y. Li, A.-g. Tang and Y.-p. Ren, *Clin. Biochem.*, 46 (2013) 1074.
12. M. S. Alonso, L. L. Zamora and J. M. Calatayud, *Talanta*, 60 (2003) 369.
13. L. Zhang, M. Song, Q. Tian and S. Min, *Sep. Purif. Technol.*, 55 (2007) 388.
14. M. Michaud, E. Jourdan, C. Ravelet, A. Villet, A. Ravel, C. Grosset and E. Peyrin, *Anal. Chem.*, 76 (2004) 1015.
15. H. Maher, N. Alzoman and S. Shehata, *Luminescence*, 32 (2017) 149.
16. Y. Huang, X. Jiang, W. Wang, J. Duan and G. Chen, *Talanta*, 70 (2006) 1157.
17. N. Jaiswal and I. Tiwari, *Anal. Methods.*, 9 (2017) 3895.
18. C. W. Foster, J. P. Metters, D. K. Kampouris and C. E. Banks, *Electroanal.*, 26 (2014) 262.
19. Q. Xu and S.-F. Wang, *Microchimica Acta*, 151 (2005) 47.
20. F. Tian, H. Li, M. Li, C. Li, Y. Lei and B. Yang, *Microchimica Acta*, 184 (2017) 1611.
21. H. Beitollahi and F. Garkani Nejad, *Electroanal.*, 28 (2016) 2237.
22. Z. Wei, Y. Yang, X. Xiao, W. Zhang and J. Wang, *Sensors Actuators B: Chem.*, 255 (2018) 895.
23. G. Das and H. H. Yoon, *Japanese Journal of Applied Physics*, 54 (2015) 06FK01.
24. M. Cano, B. Palenzuela and R. Rodríguez-Amaro, *Electroanal.* 18 (2006) 1727.
25. R. Pauliukaite, A. Malinauskas, G. Zhylyak and U. E. Spichiger-Keller, *Electroanal.*, 19 (2007) 2491.
26. M. Opallo and A. Lesniewski, *J. Electroanal. Chem.*, 656 (2011) 2.
27. X. Mei and J. Ouyang, *Langmuir*, 27 (2011) 10953.
28. T. Fukushima, *Polym. J.*, 38 (2006) 743.
29. L.-G. Zamfir, L. Rotariu and C. Bala, *Biosens. Bioelectron.*, 46 (2013) 61.
30. Y. Wang, S. Wang, L. Tao, Q. Min, J. Xiang, Q. Wang, J. Xie, Y. Yue, S. Wu and X. Li, *Int. J. Electrochem. Sci.*, 11 (2016) 2360.
31. I. Ivanov, T. Vidaković-Koch and K. Sundmacher, *J. Electroanal. Chem.*, 690 (2013) 68.
32. M. Pięk, R. Piech and B. Paczosa-Bator, *J. Electrochem. Soc.*, 165 (2018) B60.
33. R. Katakay, M. Bryce, L. Goldenberg, S. Hayes and A. Nowak, *Talanta*, 56 (2002) 451.
34. P. Calvo-Marzal, K. Y. Chumbimuni-Torres, N. F. Höehr, G. de Oliveira Neto and L. T. Kubota, *Sensors Actuators B: Chem.*, 100 (2004) 333.
35. C. D. Jaeger and A. J. Bard, *J. Am. Chem. Soc.*, 101 (1979) 1690.
36. B. Chen, Y. Zhang, L. Lin, H. Chen and M. Zhao, *J. Electroanal. Chem.* 863 (2020) 114052.
37. Q. Ma, S. Ai, H. Yin, Q. Chen and T. Tang, *Electrochim. Acta*, 55 (2010) 6687.
38. J. Zou, D. Mao, A. T. S. Wee and J. Jiang, *Appl. Surf. Sci.*, 467 (2019) 608.
39. J. Zhou, Q. Chen, Y. Wang, Q. Han and Y. Fu, *Electrochim. Acta*, 59 (2012) 45.
40. S. B. Revin and S. A. John, *Sensors Actuators B: Chem.*, 161 (2012) 1059.
41. M. Behpour, M. Meshki and S. Masoum, *J Nanostruct.*, 3 (2013) 243.
42. J. Wei, J. Qiu, L. Li, L. Ren, X. Zhang, J. Chaudhuri and S. Wang, *Nanotechnology*, 23 (2012) 335707.